

Manufacturing Process of Low-Contamination Titanium Foam as Implant Material for Cranioplasty Based on Replica Technique

Peter Quadbeck,* Ulrike Jehring, Hans-Dietrich Böhm, Alexander Füssel, and Gisela Standke

The article investigates the development of a manufacturing route for highly porous titanium foams suitable for craniofacial surgery applications, particularly in cranioplasties. The study focuses on the polyurethane replication method for foam production and emphasizes reducing residual gas content, as it significantly affects the mechanical properties and suitability for approval of the foams. Various factors such as starting materials, solvent debinding, heating schedules, and hydrogen atmosphere are analyzed for their impact on residual gas content. It is shown that significant reductions in residual gas content can only be achieved by reworking each step of the process. A combination of initial solvent debinding of the PU template with dimethyl sulphoxide, reduction of suspension additives, use of coarser Gd. 1 powders, and an integrated debinding and sintering process under partial hydrogen atmosphere achieves a significant reduction in residual gas content. This way, the potential for producing titanium foams that comply with relevant standards for craniofacial implants is demonstrated.


1. Introduction

The use of porous titanium-based structures in craniofacial surgery and especially in the area of cranioplasties has proven to be

P. Quadbeck
Peter Osypka Institute for Medical Engineering
Offenburg University of Applied Sciences
Badstr. 24, 77562 Offenburg, Germany
E-mail: peter.quadbeck@hs-offenburg.de

U. Jehring, H.-D. Böhm
Branch Lab Dresden
Fraunhofer Institute for Manufacturing Technologies and Advanced Materials IFAM
Winterbergstr. 28, 01277 Dresden, Germany

A. Füssel, G. Standke
Department Carbide Ceramics and Cellular Ceramics
Fraunhofer Institute for Ceramic Technologies and Systems IKTS
Winterbergstr. 28, 01277 Dresden, Germany

 The ORCID identification number(s) for the author(s) of this article can be found under <https://doi.org/10.1002/adem.202301392>.

© 2023 The Authors. Advanced Engineering Materials published by Wiley-VCH GmbH. This is an open access article under the terms of the Creative Commons Attribution License, which permits use, distribution and reproduction in any medium, provided the original work is properly cited.

DOI: 10.1002/adem.202301392

very reasonable.^[1] In particular, the aspects of an improved ingrowth behavior of the bone margins and the simple, safe, and fast fixation of the implant in the contact area to the bone through self-retaining forces come into play. In orthopedics, the application of such porous metals has been discussed since the late 1970s. The use of porous metals is supposed to allow an adaptation of the stiffness and strength in particular to the properties of the bone.^[2–4] In addition, such highly porous titanium foams have a very low thermal conductivity of $0.4\text{--}0.8\text{ W m}^{-1}\text{ K}^{-1}$.^[5] This property is favorable for use as a cranioplastic implant, since a higher thermal conductivity leads to greatly increased cold pain sensation in the patient. Recently, additive processes have often been used for the adjustment of porous structures, mainly because of the extensive freedom in design and structur-

ing.^[6] Selective electron beam sintering^[7] and laser sintering^[8] are particularly relevant here. These technologies are now regularly used for the production of customized implants.^[9]

Common to all CAD/CAM techniques is the long lead time of typically 1 and 2 weeks for design and fabrication, within which it is not uncommon for changes in the bone margins to necessitate further machining. Due to the manufacturing time, there is still a need for intraoperative processing. However, these additively manufactured sponges are not sufficiently adapted to the requirements of intraoperative machinability due to their relatively low porosity of typically 55–65%. However, to ensure good machinability the sponge structures must have particularly high porous properties with rather low strength of the cell struts.

Therefore, the focus here was on non-generative processes that allow the realization of even higher porosities with favorable manufacturing costs. In principle, numerous manufacturing methods are known for the production of highly porous metallic components,^[10] and numerous authors have published on the realization of titanium foams in the last 20 years.^[11,12] The suspension molding method of polyurethane sponges, also known as the Schwartzwalder method, appears to be particularly suitable for the production of osteointegrable foams. On the one hand, this method allows the realization of particularly high porosity and, on the other hand, enables cost-efficient production.

The production of titanium foams with this method has been described by various authors. For example, Li et al. report the production of components based on Ti6Al4V with 89% porosity.^[13] The authors report residual contaminations of 0.4% carbon, 0.3% oxygen, and 0.1% nitrogen of the sintered components. Similar contents of 0.33% C, 0.29% O, and 0.04% N were also achieved by the team publishing here with foams made of Ti6Al4V.^[14] Manonukul et al. produced foams based on technically pure titanium with porosities of 86–92% and cell widths of 40 ppi.^[15] In this case, the carbon content is 0.47% and the oxygen content 0.3%; no statement is made about the nitrogen content. The absorption of oxygen, carbon, and nitrogen during heat treatment is therefore a particular challenge of the process. Such contaminations have a strong influence on the strength and ductility of titanium.

For the above-mentioned intraoperative machinability, a good bendability of the cell struts and thus a good bendability of the base material is a prerequisite. With technically pure titanium as the base material, the degree of contamination with residual oxygen, carbon, and nitrogen is the central aspect. The concept of oxygen equivalent was therefore used as a suitable criterion for sufficient formability.^[16] This value includes a combined weighted summation of the C, O, and N contents with $2/3 \cdot C_C + 1 \cdot C_O + 2 \cdot C_N$. In this concept, sufficient ductility is assumed for technically pure titanium at a value of $<0.5\%$.^[17]

Another important goal in the development of titanium foams is the realization of compositions within the limits set by the DIN 17 850 and ASTM F67 standards for commercially pure titanium. The reason for this requirement is primarily a regulatory one: In the simplest case, approval of implants is obtained by demonstrating compliance with industrial standards. If such standards are met, there is a presumption of compatibility with the general safety and performance requirements of the Medical Device Regulation. Compliance with these standards is therefore an essential part of the specifications for the development of such materials. For the material developed here, a titanium grade 2 composition with a maximum concentration of 0.08% carbon, 0.25% oxygen, and 0.03% nitrogen was aimed for.

The present work deals with suitable manufacturing methods, the development of which is described in the Results section. The focus is primarily on the reduction of the residual gas content. Initially, moderate porosities in the range of 90% were set. The increase of the porosity to 95% as well as the optimization of the elongation and bendability are dependent on numerous other parameters, in a complex way, and will therefore be the subject of later publications.

2. Experimental Section

Commercially pure titanium was used as the base material. Three different powders with different degrees of purity were used. A very fine powder with grade 2 (TLS Technik, Germany) shows powder sizes of $d_{50} = 6.6$ and $d_{90} = 9.4 \mu\text{m}$ with a standard deviation of $1.9 \mu\text{m}$. A slightly coarser powder with the same grade (AP&C, Canada) has powder sizes of $d_{50} = 10.7$ and $d_{90} = 16.4 \mu\text{m}$ with a standard deviation of $3.9 \mu\text{m}$, and finally a coarser powder with Grade 1 (AP&C, Canada) was used with particle sizes of $d_{50} = 26.7$ and $d_{90} = 44.0 \mu\text{m}$ with a standard deviation of $7.6 \mu\text{m}$. **Figure 1** shows the distribution of these powders used.

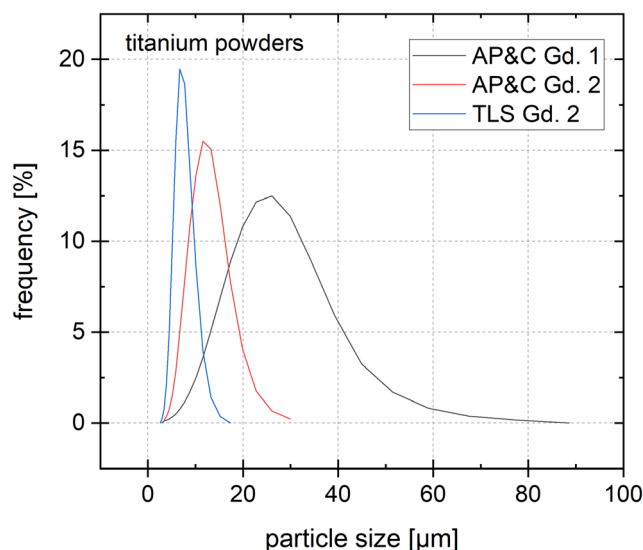


Figure 1. Particle size distribution of the used titanium powders.

Table 1. Residual gas contents and oxygen equivalent of the used titanium powder.

Powder	Oxygen [%]	Carbon [%]	Nitrogen [%]	Oxygen equivalent [%]
TLS Gd. 2	0.298	0.010	0.020	0.35
AP&C Gd. 2	0.229	0.019	0.034	0.31
AP&C Gd. 1	0.142	0.005	0.002	0.15

The residual gas contents of these powders determined by elemental analysis are shown in **Table 1**. It is noticeable that the residual contaminations of both powders designated as grade 2 are nominally in the range of a grade 3 powder, whereby the oxygen content is significantly increased in the TLS powder and the nitrogen content is slightly increased in the AP&C powder.

The titanium foams produced in the present work are based on the Schwartzwalder method. The state of the art with this process is the coating of polyurethane foams with a suspension of metal powder, temporary binder, process aids and rheological additives. The suspension is impregnated into the foam template and excess material is removed by a rolling process. Afterwards samples are dried. The organic component is removed in a debinding furnace, after which the parts are transferred to a sintering furnace and the metal powder skeleton is sintered.

The developmental process was carried out with different suspension formulations. The main formulations have the compositions shown in **Table 2** as the starting point and end point of the development. The first suspension contains a total of 6% additives consisting of carbon, oxygen, and nitrogen compounds, which can react to form titanium carbides, oxides, or nitrides during the subsequent heat treatment. The second formulation is a suspension reduced to a total of 2.1% additives with modified dispersing aids and reduced defoamer proportions.

Polyurethane sponges are usually used as template material in the Schwartzwalder process. In addition to the suspension

Table 2. Raw materials and composition of the suspension used for the impregnation of the PU foams.

	Suspension 1		Suspension 2	
	Chemical composition	Mass [%]	Chemical composition	Mass [%]
Powder	TLS Technik Gd. 2	100	AP&C Gd. 1	
Dispersing additive	Carboxylic acid, alkaline adjusted	0.325	Amino alcohole	0.45
Defoamer 1	Stearic acid, silica acid	0.2	Stearic acid, silica acid	0.4
Defoamer 2	Siloxane	5		
Wetting additive 1			Polyurethane	
Wetting additive 2	Polyurethane	0.12	Ester	0.415
Rheological addiive	Polyurethane	0.12	Polyurethane	0.12
Binder	Polysaccharide	0.2	Polysaccharide	0.2
Water		10	Water	10

additives, the polyurethane foams are the second source of impurities in the titanium sponge, as these have to be thermally degraded during the heat treatment and in turn consist of carbon, oxygen, and nitrogen. Compared to the binders, they are additionally present in a larger quantity and thus have an even greater influence on the sintering result. For this reason, white polyurethane foams, not colored with carbon black, were used on the one hand. On the other hand, polyurethane foams based on polyether were used, which have a simpler chain structure without double bonds compared to polyester foams (Recticel Engineered Foams, Germany). The equivalent cell width of the large cell of this template was 1700 μm . Specimens with dimensions of $80 \times 80 \times 6$ mm were sawn from larger blocks of this material using a high-speed band saw.

The water-based suspensions have been prepared using a standard stirrer without the need for high energy dispersing. The impregnation process was performed manually. The homogenization of the coating and the removal of excess slurry were performed either by standard rolling process or a centrifugation step. The amount of slurry loaded into the foam was controlled by a scale. Particular attention has been paid for the avoidance of closed cells and cell windows and the reproducible adjustment of the foam porosity.

The solvent debinding used in the present work as an additional process step before impregnation was carried out with an in-house manufactured solvent system. This system consists of a heatable stainless steel tank, in which debinding takes place at 80 °C under constant stirring.

The heat treatment was carried out in two different furnace concepts. In concept 1, a tube furnace with a quartz glass tube of 120 mm diameter was used for debinding. Debinding was carried out under argon 6.0 at a pressure of 60 mbar and a gas flow of 101 h^{-1} . The sintering was carried out in a high-vacuum sintering furnace (Xerion, Germany) with tungsten heaters in a high-vacuum of 10^{-5} mbar. Debinding was carried out with holding stages at 240 °C/40'; 290 °C/50'; 340 °C/15', and 600 °C/10', sintering was carried out at 1350 °C/60'.

In concept 2, an integrated debinding and sintering furnace (MUT Advanced Heating GmbH, Germany) was used. This system consists of a double-wall furnace, whereby the inner part is used as a hot-wall furnace during debinding and as a cold-wall furnace during sintering (furnace-in-furnace principle). Argon

6.0 and hydrogen 6.0 were used for the process, the parameterization can be found in the section "Results".

The porosity of the titanium foam moldings was measured by measuring the outer geometry of the moldings using calipers and relating the volume thus determined to the mass of the moldings. With a measurement accuracy of ± 0.5 mm, the porosity can thus be determined to within $\pm 1.2\%$.

The analysis of residual carbon, oxygen, nitrogen, and hydrogen content after heat treatment was carried out for carbon on a LECO CS230 and for oxygen, nitrogen, and hydrogen on a LECO TCH600 instrument. The particle size was analyzed by laser diffraction on an LA950 from Horiba.

In order to observe the gas composition during the process, in-situ gas phase observation was carried out by Fourier-transform-infrared spectroscopy (FTIR), using a ThermoFisher Scientific Antaris IGS. The infrared beam from the broadband IR source first passes through a mirror system and enters the tube furnace via KBr windows. On the opposite side of the tube, the signal again passes a KBr window and is finally detected by an external mercury-cadmium-telluride photodetector. Characteristic spectra were taken from a database as a reference. Thus, single species could be identified. Spectra were taken in temperature steps of 3 K. The relative concentration of the observed species was determined by drawing a baseline between two defined fixed points and integrating the area between the baseline and the measured absorbance. The measurements were carried out in an alumina tube with an Ar 6.0 atmosphere of 1 bar as well as with a quartz tube with an Ar 6.0 atmosphere of 60 mbar. The method has been described in detail in ref. [18].

Furthermore, an attenuated total reflection (ATR) infrared spectroscopy device (Alpha Bruker Optics, Germany) was used to detect the impact of solvent debinding on the PU template.

Finally, it should be noted that in the present publication, percentages of residual contaminations always describe the composition of the material. This means, in particular, that differences in residual gas contents always represent differences in contents, not percentage changes of the material composition.

3. Results

The standard process defined above, which was carried out with suspension 1 and separated heat treatment, initially serves as a

reference. This process produces titanium foams with porosities of 90–92%, which have an oxygen content of $0.65 \pm 0.04\%$, a carbon content of $0.54 \pm 0.13\%$ and a nitrogen content of $0.12 \pm 0.04\%$. From this, an oxygen equivalent of $1.26 \pm 0.07\%$ can be calculated.

3.1. Effect of Starting Materials

An immediately understandable and significant influence on the residual gas content is the residual gas content of the starting powder used. For example, the use of AP&C's grade 2 powder reduces the oxygen equivalent of the sintered part by about 0.07% compared to the TLS powder, which corresponds approximately to the reduced initial content within the possible measurement accuracy. When using the coarser grade 1 powder from AP&C, the reduction of the oxygen equivalent of about 0.31% is significantly greater than the initial values of the residual gas contents suggest. The reduction of the oxygen equivalent is mainly due to reduced oxygen contents (-0.19%) and carbon contents (-0.13%). In addition to the lower contamination, the advantage of these powders is primarily a reduced surface-to-volume ratio of the coarser powder, which results in reduced absorption of the gases.

In the Schwartzwalder coating technology, polyurethane sponges colored with carbon black solutions are typically used. Measurements with the residual gas content with standard heat treatment show an oxygen content reduced by 0.02% and a carbon content reduced by 0.07% when using the white PU foam. Furthermore, the use of a polyether foam as template material results in a 0.1% reduction of the oxygen equivalent. The influence of the reduced organic content could not be quantified due to complex overlapping effects.

3.2. Effect of Solvent Debinding

The solvent debinding that precedes the thermal debinding serves to reduce organic components on the one hand, and on the other, to change molecular structures for improved thermal pyrolysis. When debinding polyurethane sponges coated with titanium powder, treatment with acetone leads to washing off the coating. Therefore, the solvent treatment of the polyurethane sponges was carried out before coating. A suitable solvent must change the chemical structure of the polyurethane to such an extent that thermal decomposition is shifted to lower temperatures and maintain the mechanical stability of the foam so that subsequent coating remains possible. To determine a suitable solvent, a screening was carried out with uncoated foams with acetonitrile, acetylacetone, benzene, butyl acetate, chloroform, cola, cyclohexanone, diesel, dimethylformamide, ethyl acetate, isopropanol, tetrahydrofuran, toluene, petroleum ether, xylene, and dimethyl sulphoxide (DMSO). On the one hand, the mass change and on the other hand, structural analyses were carried out by means of ATR infrared spectroscopy. As a result, **Figure 2a** shows essentially similar spectra for all solvents. Only when treated with DMSO for 2×1 h at 80°C there is a significant decrease in mass of 10%. In the ATR spectrum, significant structural changes are only visible for DMSO in the comparison of the structures before and after treatment, especially in the wavelength range of 1800 and 1000 cm^{-1} . Diesel, benzene, and acetonitrile show some impact on the intensity of the peaks, but not on their appearance in terms of wave number. Thus, only DMSO shows significant structural and mass changes with solvent debinding.

The effect of this pre-treatment on the debinding process under Ar 6.0 at 1 bar is shown by the FTIR in-situ gas analysis. In this context, **Figure 2b** depicts the integrated absorbance areas

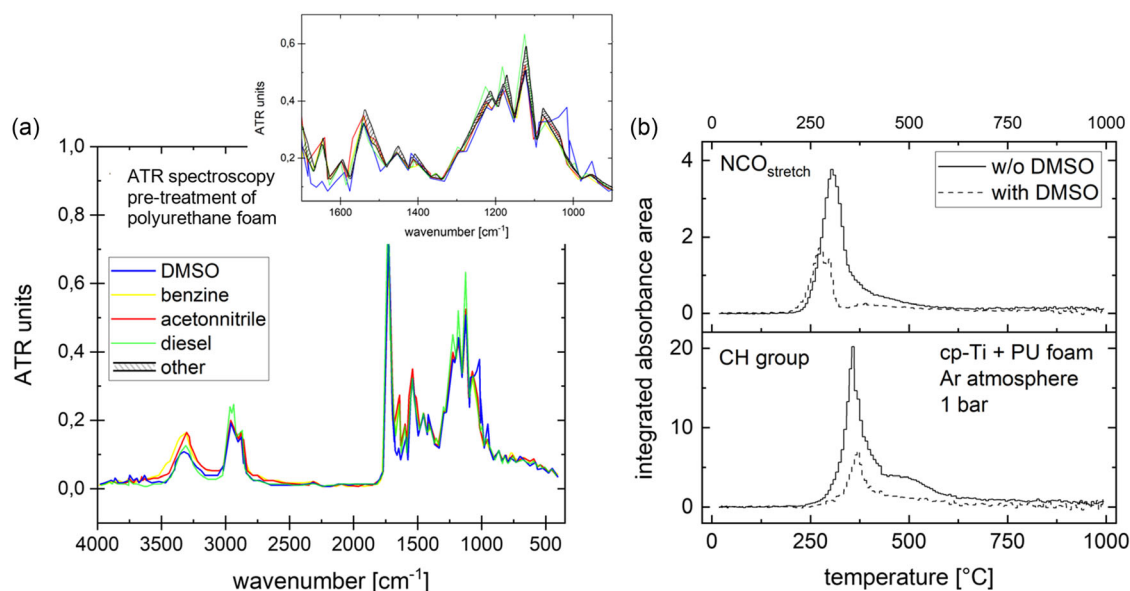


Figure 2. a) ATR-infrared spectroscopy of polyurethane foams pre-treated with various solvents. The upper inserted diagram shows the relevant region between 1700 and 900 cm^{-1} . DMSO is the only solvent that has a distinct effect on the polyurethane foams. b) shows in situ FTIR gas analysis of the released gases during the debinding of the suspension coated PU foams with and without DMSO-pre-treatment.

of the released CH group species as well as the NCO gases, which have been calculated by the spectra recorded at different temperatures. These species are the predominant released gases during the debinding step and therefore indicate the decomposition of the organic fractions. The figure shows the difference in the gas evolution of these two species with and without DMSO pretreatment. As a result, a reduced gas release of both gases can be observed. Particularly noteworthy is the lower decomposition temperature of the NCO gases, which is mainly due to the decomposition of the polyurethane molecular chains. Here, solvent debinding has a measurable influence on the decomposition mechanisms. The effect of this procedure on the residual gas contents can be determined after sintering. Therefore, samples produced in this way and samples that had not been pre-treated were thermally debinded as well as the remaining residual contaminations were determined. As a result, an oxygen content reduced by 0.1% and a carbon content reduced by 0.15% were determined.

During this pre-treatment, the polyurethane sponges undergo significant reversible swelling. Since this swelling would lead to flaking of the coating, the solvent debinding of the bare polyurethane sponges has to take place as a pre-treatment. Only after subsequent drying are the pre-treated structures coated with metal powder suspension. **Figure 3** illustrates the impact of solvent debinding with DMSO on the white polyurethane foam. In comparison to the untreated foam (**Figure a**), a significantly lower opacity of the material can be observed after the treatment (**Figure b**), indicating an increase in scattering centers due to the breakdown of the chemical structure. Additionally, the above-mentioned swelling effect is noticeable, resulting in a slightly increased thickness of the cell struts.

3.3. Effect of Heating Schedule

Heat treatment with separate debinding and sintering is state of the art. This treatment shows that a large proportion of the residual gases is introduced by the decomposition products produced during debinding. Nevertheless, sintering also significantly increases the residual gas content by an oxygen equivalent of 0.44%. The pick-up from residual oxygen of the protective gas accounts for the largest share with about 0.26%, but the carbon content also increases by 0.15% on average during sintering.

After debinding, this conventional process requires cooling of the furnace, transfer of the components through the ambient air

and reheating in the sintering furnace. These steps induce additional contamination, especially with oxygen. To avoid this effect, the heat treatment was carried out in an integrated debinding and sintering furnace. The advantage of this procedure is the elimination of the above-mentioned cooling and heating time as well as the transfer of the samples with air contact. For this purpose, the already developed regime had to be modified in such a way that a constant temperature gradient is applied between the inner and outer furnace. Such a gradient is necessary so that the debinding gases run from the inner part to the outer area and gas diffusion from the outside to the inside is prevented accordingly.

To determine a suitable regime, FTIR in-situ gas analysis measurements were carried out in Ar atmosphere at 60 mbar with a constant heating rate of 3 K min⁻¹. For reasons of space, we do not show the spectra measured at temperature steps of 3 K. From these spectra, the integrated absorbances of the respective species were calculated (see method section). The most significant species in these measurements are the CH group on the one hand and the NCO molecules on the other. As a result, **Figure 4** shows the occurrence of NCO and CH group molecules as a function of sample temperature with maxima at 250 and 310 °C, respectively. This means that the corresponding species are released at this temperature as a result of decomposition of the PU template and the suspension additives. As a result, **Figure 4** shows the values of the CH group as well as the NCO species, which are predominant in the decomposition spectra. As depicted, the decomposition of the polyurethane template into NCO molecules takes place at temperatures of about 250 °C. The decomposition of the backbones (binder/binder aid/template) into the CH group as well as into alcohol occurs with a peak at 310 °C. Consequently, the temperatures of 250 and 310 °C are important holding points for debinding, because this is where the strongest decomposition activities take place. At about 400 °C, the decomposition activities are largely completed.

Based on this data, the initially realized regime of the integrated debinding and sintering cycle is shown in **Figure 5a**. This schedule includes debinding up to 400 °C at 60 mbar and sintering in high vacuum (5×10^{-5} mbar). The individual temperature stages are clearly smeared by the heater arrangement of the furnace-in-furnace design of the integrated debinding and sintering furnace. With such regimes, reductions in oxygen equivalents of about 0.13% are achieved with an occupancy of 4–6 samples per cycle.

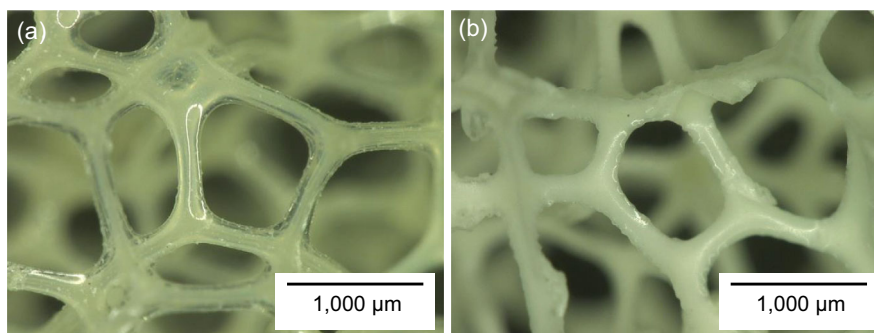


Figure 3. a) Comparison of PU foam prior and b) after DMSO treatment.

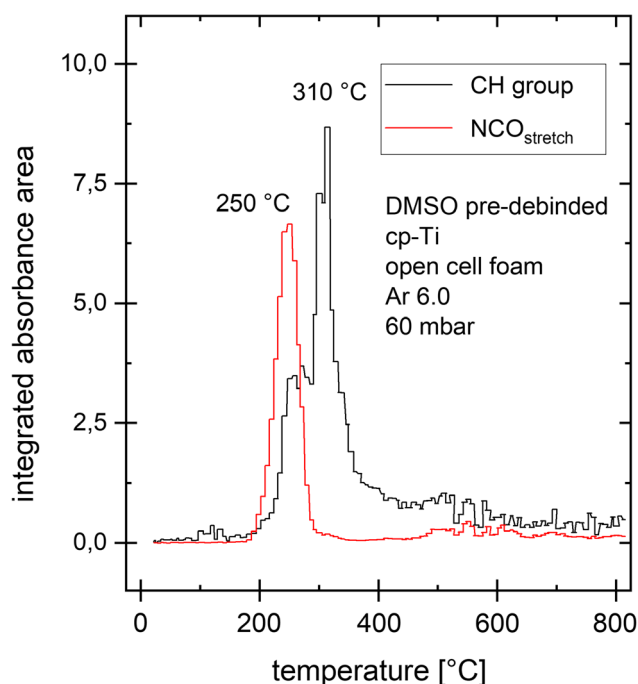


Figure 4. In situ FTIR gas phase analysis during debinding of DMSO-pre-debinded titanium foams in Ar 6.0 atmosphere with pressure of 60 mbar. Distinct peaks of the NCO stretch signal, and the CH group indicate the main decomposition activity at 250 and 310 °C.

3.4. Effect of Hydrogen Atmosphere

From debinding analysis of the heat treatment of steel components, it is known that decomposition under 100% hydrogen occurs at low temperatures in the decomposition phase within smaller process windows in comparison to treatment in inert atmospheres. In addition, at high temperatures a carbon reduction can be achieved by methane formation.^[19] Furthermore, hydrides may reduce impurities during sintering of titanium.^[20]

In order to realize debinding of titanium components, the phase of titanium hydride formation between 300 and 600 °C must be bridged. For this purpose, the integrated debinding/sintering furnace was operated up to 200 °C under H₂, in the range up to 900 °C under argon 6.0 and above this again under H₂ 6.0, taking safety reserves into account. During cooling, argon 6.0 was then reintroduced in the range of 1030–350 °C. The whole process was conducted at 60 mbar pressure, with a temperature schedule as shown in Figure 5b. In this way, the oxygen equivalent was reduced by about 0.29%. The hydrogen content of this way treated samples is 0.003%, which represents an unchanged value compared to the used titanium grade 1 powder. We can therefore rule out embrittlement caused by the hydrogen atmosphere. Interestingly, not only the carbon content but also the oxygen and nitrogen contents were reduced. Thermodynamically, a reduction of titanium oxides in particular is not possible in this temperature and pressure range. It can therefore be assumed that the polymer decomposition temperature is reduced under hydrogen and after DMSO pretreatment.

In addition, the entire cycle was shortened to reduce oxygen uptake. In order to still obtain densely sintered samples, the sintering temperature was increased by approx. 40 K. Overall, the course shown in Figure 5b was realized. The result for all critical gases (C/N/O) is a significant reduction of the oxygen equivalent by about 0.09%.

With the measures and modified starting materials presented here, titanium foams with an oxygen content of 0.23%, a carbon content of 0.14%, and a nitrogen content of 0.03% were finally produced. The oxygen equivalent of these parts is 0.38%. **Figure 6a** shows the image of such a sintered titanium foam. Porosity was determined by measuring the entire sample to a value of 90.7% as described in the methods section. Details of the surface of this sample are shown in Figure 6b. In particular, the picture shows the typical structure of the foam, in which the majority of the cell windows are open. Occasionally, closed cell windows can be seen (indicated by an arrow), which result from the suspension coating process. By optimizing the composition shown in Table 2, the proportion of closed cell windows was kept

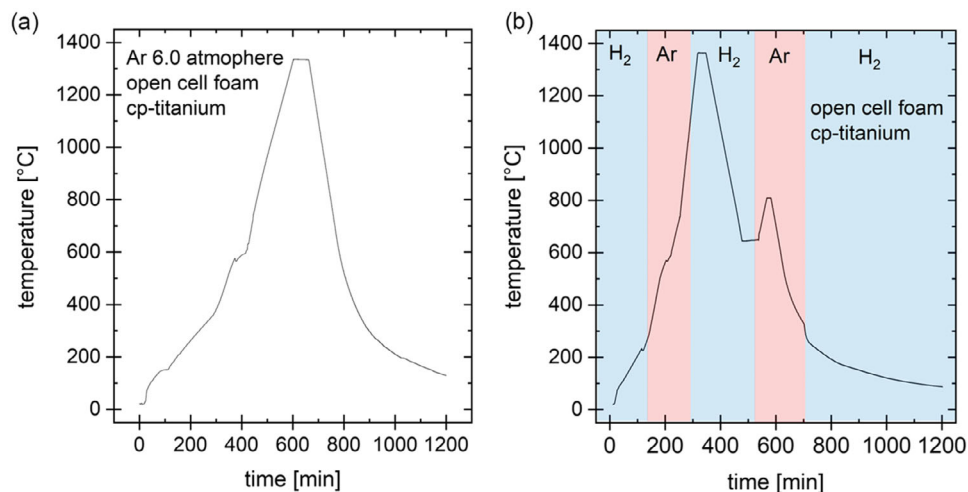


Figure 5. a) Heating schedule of the integrated debinding and sintering of titanium foams in inert Ar atmosphere and b) accelerated heat treatment schedule with the partly introduction of 100% hydrogen atmosphere.

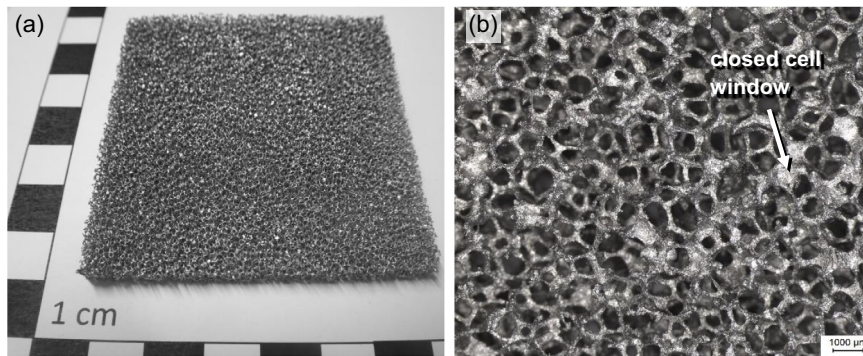


Figure 6. a) Picture of a sintered titanium foam and b) surface of the same, produced with the optimized process schedule.

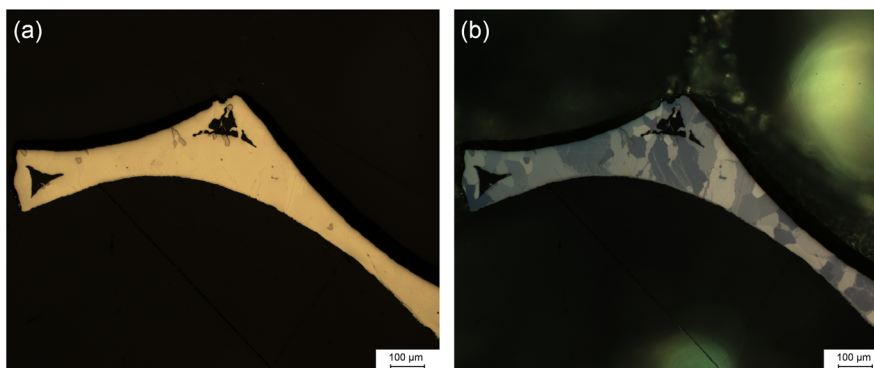


Figure 7. Light microscopical image of the cross section of a strut of PU-based titanium foams. a) The struts show nearly full density, and after etching b) the grain size is visible, which is larger than the particle size of the starting powders.

very low. However, these closed cell windows were not quantified. Finally, the samples were examined metallographically. **Figure 7** shows light microscopic images of unetched and etched structures. Here, the sections initially show a microporosity of the cell struts approaching zero. The larger triangle-shaped areas correspond to the position of the removed polyurethane sponges. In the etched state, the individual grains can also be seen. The figures show that the grain size is on average significantly larger than the size of the initial powders (see Figure 1). This shows that a relevant grain coarsening is produced by the sintering. It is known from the literature that fine-grained titanium alloy microstructures can be produced by the partial use of hydrogen during heat treatment.^[21] Therefore, the grain sizes of the titanium foam samples were tested after the sintering under hydrogen described above. The investigation of the etched samples (Figure 7b) shows that such a grain refinement effect could not be achieved with the titanium foams using the described regime.

4. Discussion

A summary of the reductions achieved through measures of targeted of raw materials and process modifications is shown in **Table 3**. If the individual effects are added up linearly, an oxygen equivalent of 0.12 could be achieved. This shows that the individual measures interact in a complex way and cannot be

Table 3. Summary of the reductions achieved through measures of targeted of raw materials and process modifications.

Factor	C content [%]	O content [%]	N content [%]	Oxygen-equivalent [%]
DMSO pre-biding	-0.16	-0.10	0	-0.20
White Polyether template	-0.07	-0.02	+0.01	-0.07
AP&C Gd 2 versus TLS Gd 2	-0.02	-0.12	+0.03	-0.07
AP&C Gd 1 versus AP&C Gd 2	-0.19	-0.13	-0.06	-0.31
Integrated debinding and sintering	+0.04	-0.18	+0.01	-0.13
Hydrogen heat treatment	-0.11	-0.11	-0.05	-0.29
Short heat treatment	-0.08	-0.06	+0.01	-0.09

combined in a linear fashion. The total reduction of the residual contamination is therefore lower than the sum of the individual effects.

With the oxygen equivalent set to significantly less than 0.5%, it is now expected that the bendability of the foams is given. Thus, it can be expected that sufficient plastic deformability for intraoperative machinability will be achieved. The investigation of these mechanical properties of the parts is the subject of a later publication. Overall, however, the residual gas content is still not

within the definition range, as the carbon content of 0.14% is 0.06% too high. However, it is to be expected that, from experience, a further reduction of the residual gas content will take place with the conversion of the process to larger industrial furnaces. It is therefore very likely that with the measures proposed here, a titanium foam can be produced whose chemical composition lies within the standards ASTM F67 as well as DIN 17 850. Thus, at least regarding the base materials, a considerably simplified procedure can be expected in the assessment of compatibility with the safety and performance requirements of the Medical Device Regulation MDR.

5. Conclusion

In this exploration of porous titanium foam development for craniofacial surgical applications, the reduction of residual gas content emerges as a central focus. The study modifies the known manufacturing route to produce highly porous commercially pure titanium foams that align with the requirements of intra-operative post-processing, particularly in cranioplasties. The investigation emphasizes the significance of mitigating residual gases, which impact the mechanical properties and the suitability of the material for approval as medical device.

The study demonstrates that through systematic selection of appropriate starting materials as well as pretreatment methods, along with integrated debinding and sintering, and by partially using hydrogen atmospheres, a significant reduction in residual gas contents becomes achievable. The most substantial influences are the introduction of a pretreatment of the polyurethane foams with dimethyl sulphoxide (DMSO), the use of hydrogen atmospheres at low and high temperatures, and especially the use of highly pure grade 1 titanium powders with particle sizes that are not too small. With all these measures, components with an oxygen content of 0.23%, a carbon content of 0.14%, and a nitrogen content of 0.03% were realized in the present study. These values confirm the effectiveness of the taken measures in substantially minimizing the residual gas content. It must be noted that the effects of the individual measures do not linearly accumulate, so due to mutual influences, the minimally achievable residual gas contents are higher than the sum of the individual measures. The outcome of this investigation points towards the feasibility of producing titanium foams that conform to stringent standards for craniofacial implants.

Acknowledgements

The authors are grateful to the German Ministry for Education and Research (BMBF) for funding (Grant No. 13GW0113).

Open Access funding enabled and organized by Projekt DEAL.

Conflict of Interest

The authors declare no conflict of interest.

Data Availability Statement

Research data are not shared.

Keywords

cellular metals, debinding, manufacturing process, sintering, titanium

Received: September 1, 2023

Revised: October 30, 2023

Published online:

-
- [1] J. Parthasarathy, *Ann. Maxillofac. Surg.* **2014**, *4*, 9.
 - [2] J. N. Weber, E. W. White, *Mater. Res. Bull.* **1972**, *7*, 1005.
 - [3] D. M. Robertson, L. Pierre, R. Chahal, *J. Biomed. Mater. Res.* **1976**, *10*, 335.
 - [4] H. U. Cameron, I. Macnab, R. M. Piliar, *Int. J. Artif. Organs* **1978**, *1*, 104.
 - [5] P. S. Liu, H. B. Qing, H. L. Hou, Y. Q. Wang, Y. L. Zhang, *Mater. Des.* **2016**, *92*, 823.
 - [6] D. Melancon, Z. S. Bagheri, R. B. Johnston, L. Liu, M. Tanzer, D. Pasini, *Acta Biomater.* **2017**, *63*, 350.
 - [7] P. Heintz, A. Rottmair, C. Körner, R. F. Singer, *Adv. Eng. Mater.* **2007**, *9*, 359.
 - [8] D. A. Hollander, M. von Walter, T. Wirtz, R. Sellei, B. Schmidt-Rohlfing, O. Paar, H. J. Erli, *Biomaterials* **2006**, *27*, 955.
 - [9] J. Banhart, *Prog. Mater. Sci.* **2001**, *46*, 559.
 - [10] D. Miljanovic, M. Seyedmahmoudian, A. Stojcevski, B. Horan, *Ann. Biomed. Eng.* **2020**, *48*, 2285.
 - [11] S. E. Thoulon, S. Magnin, A. I. Gomes Costa, J. Geringer, *J. Bio-Tribo-Corros.* **2023**, *9*, 48.
 - [12] G. Ryan, A. Pandit, D. P. Apatsidis, *Biomaterials* **2006**, *27*, 2651.
 - [13] J. P. Li, S. H. Li, K. de Groot, P. Layrolle, *Key Eng. Mater.* **2002**, *218–220*, 51.
 - [14] P. Quadbeck, K. Kümmel, R. Hauser, G. Standke, J. Adler, G. Stephani, B. Kieback, *Adv. Eng. Mater.* **2011**, *13*, 1024.
 - [15] A. Manonukul, P. Srikudvien, M. Tange, *Mater. Sci. Eng., A* **2016**, *650*, 432.
 - [16] H. R. Ogden, R. L. Jaffee, TML Report No. 20, Bastelle Memorial Institute, Columbus, OH **1955**, <https://doi.org/10.2172/4370612>.
 - [17] U. Zwicker, *Titan und Titanlegierungen*, Springer-Verlag, Berlin/Heidelberg **1974**, <https://doi.org/10.1007/978-3-642-80587-5>.
 - [18] A. Strauß, P. Quadbeck, H. D. Böhm, O. Andersen, T. Weißgärber, *HTM J. Heat Treat. Mater.* **2022**, *77*, 437.
 - [19] R. Oro, M. Campos, C. Gierl-Mayer, H. Danninger, J. M. Torralba, *Metall. Mater. Trans. A* **2015**, *46*, 1349.
 - [20] R. M. German, *Int. J. Refract. Met. Hard Mater.* **2020**, *89*, 105214.
 - [21] E. Guo, D. Liu, L. Wang, F. Kang, *Mater. Sci. Eng., A* **2008**, *472*, 281.